analytical chemistry

pubs.acs.org/ac Letter

Visualization of Streams of Small Organic Molecules in Continuous-Flow Electrophoresis

Nikita A. Ivanov, Sven Kochmann, and Sergey N. Krylov*

Cite This: *Anal. Chem.* 2020, 92, 2907−2910 Read Online

ACCESS | Metrics & More | Article Recommendations | Supporting Information

ABSTRACT: Continuous-flow electrophoresis (CFE) separates a stream of a multicomponent mixture into multiple streams of individual components inside a thin rectangular chamber. CFE will be able to benefit flow chemistry when it is both compatible with nonaqueous solvents utilized in organic synthesis and capable of generically detecting streams of small organic molecules. While stable nonaqueous CFE has been demonstrated, generically detecting molecular streams has not been achieved yet. Here we propose a general approach for molecular stream visualization in CFE via analyte-caused obstruction of excitation of a fluorescent layer underneath the separation chamber—fluorescent sublayer-based visualization (FSV). The concept of FSC-based visualization has been adapted from visualization of small organic molecules on fluorescent plates in thin-layer chromatography. We designed and fabricated a CFE device with one side made of quartz and another side made of UV-absorbing visibly fluorescent, chemically inert, machinable plastic. This device was demonstrated to support nonaqueous CFE of small organic molecules and quantitative detection of their streams in real-time with a limit of detection below 100 μM. Thus, CFE may satisfy conditions required for its seamless integration with continuous flow organic synthesis in flow chemistry.

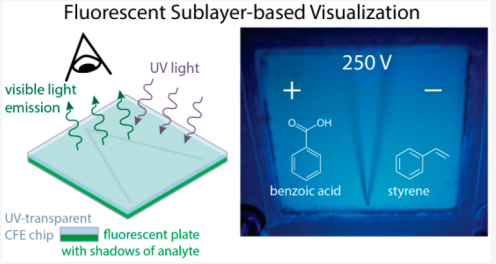

Continuous-flow electrophoresis (CFE) separates a stream of a multicomponent mixture into multiple streams of individual components inside a thin rectangular chamber with an electric field perpendicular to the hydrodynamic flow.[1−3] CFE can potentially benefit flow chemistry, which currently lacks inline multicomponent separation in a single organic phase.[4,5] To become useful for flow chemistry, CFE must be compatible with nonaqueous solvents utilized in organic synthesis and capable of generically detecting multiple molecular streams of small organic molecules in real-time. While stable nonaqueous CFE (NACFE) has been demonstrated,[6,7] generically detecting molecular streams in real-time has not been achieved yet. Detection of streams in CFE usually relies on analyte fluorescence;[8−14] however, fluorescence is not a universal property of molecules. Mass spectrometry (MS) is a generic detection approach, but it can only be interfaced with CFE offline,[15−17] and, thus, cannot detect multiple molecular streams in real-time. In addition, a mass-spectrometer is prohibitively expensive as an on-board detector in CFE. Our current work was motivated by the insight that being a very common feature of organic molecules, UV absorbance in the range of 200−300 nm can potentially be a basis for a generic way of real-time detection of multiple streams of small organic molecules in CFE.

UV detection of streams in a mesoscale CFE chip (with a separation chamber dimensions being in the order of 5 cm × 5 cm × 0.2 mm) is not a trivial task. The most straightforward approach is to use UV absorbance imaging with a UV-transparent CFE chip positioned between a UV light source and a UV camera (Figure 1A). This approach is very expensive as it requires a difficult-to-make all-quartz chip, expensive UV optics, and a very expensive UV camera. The high cost of this solution will most likely make it prohibitive for practical use. Here we propose a more elaborate but much less expensive alternative to UV absorbance imaging, namely, a well-known approach of stream visualization via analyte-caused obstruction of excitation of a fluorescent sublayer placed underneath the separation chamber.[18−24] Conceptually, a source of UV light and a visible-range camera (or the naked eye) are positioned on one side of the CFE chip while a sublayer capable of fluorescing in the visible range upon UV excitation is positioned on the opposite side (Figure 1B). If an analyte in the CFE chip absorbs UV light, it decreases intensity of UV light reaching the sublayer and, thus, decreases fluorescence intensity from the shadowed area. Additionally, fluorescence is visible to the naked eye and, thus, in principle, no camera is needed provided that the eye is protected from stray UV light. This fluorescence-mediated visualization approach was invented in 1947 and has been successfully used since then to detect small organic molecules in thin-layer chromatography (TLC).[18,19] It was later adapted for detection of nucleic acids in gel electrophoresis.[20−24] In TLC, separation of organic

Received: December 19, 2019
Accepted: January 28, 2020
Published: January 28, 2020

https://dx.doi.org/10.1021/acs.analchem.9b05734
Anal. Chem. 2020, 92, 2907−2910

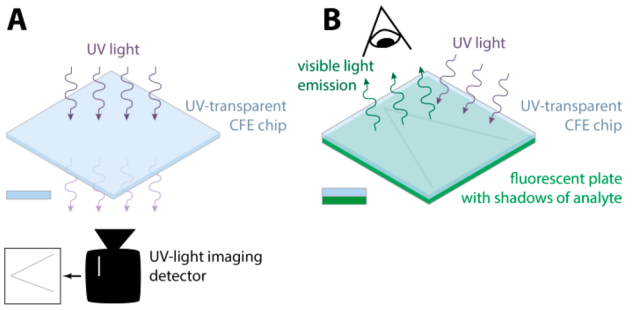

Figure 1. Schematics of UV imaging using UV optics and UV camera (A) and fluorescent sublayer visualization (FSV) (B). (A) UV light passes through the transparent CFE chip in which analytes absorb some of the UV light. A UV camera positioned on the opposite side of the chip images UV shadows created by the UV-absorbing streams. (B) UV light passes through the transparent CFE chip in which analytes absorb some of the UV light. The remaining UV light excites fluorescence of a UV-absorbing visibly fluorescent plate positioned on the opposite side of the chip. Absorption of UV light by the analytes decreases fluorescence in the shadowed areas. UV-absorbing molecular streams are visible to the naked eye or a common photo/video camera as dimmer areas on a bright fluorescence background.

molecules occurs right on the fluorescent TLC plate making their fluorescence-mediated visualization trivial. Using a fluorescent sublayer for visualizing nucleic acids within the gel is also simple as it only requires that a UV-transparent gel be placed on a fluorescent plate, e.g., a TLC plate. Using a fluorescent sublayer for stream visualization in CFE is much more complicated as the streams are within a CFE device. Accordingly, the whole device should be placed on the fluorescent plate, and the device should, thus, be UV-transparent. Such requirements impose significant technical challenges in CFE-device fabrication and optical-setup design. The goal of our work was to find a practical solution for these technical challenges and prove the feasibility of visualizing molecular streams in CFE using attenuated fluorescence of a fluorescent sublayer.

The technique of visualizing UV-absorbing species using a fluorescent sublayer requires a descriptive name. No such name was introduced when it was invented and applied to TLC.[18,19] When the technique was adopted for visualizing nucleic acids in gels, it was termed UV shadowing.[20−24] We find this term nondescriptive; in essence, it is equivalent to the general term of UV absorbance. As a result, UV shadowing cannot distinguish between the two different techniques of visualization shown in Figure 1. In both techniques, UV-absorbing species create a UV shadow: on a camera in Figure 1A and on a fluorescent sublayer in Figure 1B. Accordingly, for an approach utilizing fluorescence, we suggest the descriptive term fluorescent sublayer-based visualization (FSV).

We have previously developed an imaging system and image-analysis software for detection and characterization of streams of fluorescent analytes in CFE.[10,25] In principle, FSV could utilize the same setup and software provided that the visible-range fluorescence−excitation light source be replaced with a UV one. However, for this work we assembled a new setup with a common hand-held UV-lamp (254 nm) and a mirrorless micro-four thirds camera as the detector (Figure 2). We did this because our previous setup uses a light emitting diode (LED) as the light source, and we could not find a sufficiently powerful LED (>10 mW) for UV excitation. The

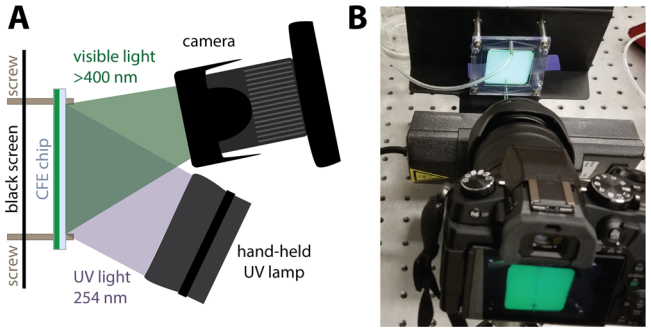

Figure 2. Schematic (A) and photo (B) of the FSV setup designed, assembled, and used in this work. The chip is mounted against a black background. A customary hand-held UV lamp (254 nm main band excitation) is used as a UV light source and a mirrorless camera (Panasonic Lumix DMC-G85 with a 12−60 mm objective; UV and polarization filter) is used as a detector for visible-light fluorescence of the fluorescent sublayer (>400 nm).

hand-held UV lamp which we used in the new setup had a bright bulb with a 254 nm main band excitation (4 W of lamp power consumption), but it required a new arrangement of the optical components.

To demonstrate that FSV is a practical stream-visualization method for nonaqueous CFE, we aimed to reliably image organic molecules in our mesoscale CFE device with a 200 μm thickness (height) of the separation chamber.[6] As CFE should benefit flow chemistry and flow chemistry deals with relatively high concentrations in the millimolar range,[4,5] our goal was to achieve a sub-millimolar LOD (concentration providing a signal-to-noise ratio of 3) in a 200-μm-thick CFE chamber. Additionally, we considered a set of *a priori* options for device design with three criteria in mind: (i) feasibility of device fabrication, (ii) UV transparency of the device, and (iii) chemical inertness of device material (Table 1). Our procedure

Table 1. Chip Assemblies and Properties for Various Combinations of Quartz, Transparent Plastic (TP), and Fluorescent Plastic (FP)

	top	bottom	TLC plate required	optical clarity[a]	machinability[b]	chemical resistivity[c]
1	quartz	quartz	yes	●●●	●	●●●
2	TP	TP	yes	●	●●●	●●
3	quartz	TP	yes	●●	●●●	●●
4	quartz	FP	no	●●●	●●●	●●

[a]Optical clarity in the UV-region (200−300 nm) of the optical spectrum. [b]Ability to mill plastics using our established protocols for PVC.[6] [c]Compatibility with propylene carbonate.

for fabricating a mesoscale CFE device with a large-area (5 cm × 5 cm) but a shallow (200 μm) separation chamber involves machining the bottom and top pieces of the device and bonding both pieces together; machining the top piece can be avoided if the material possesses an even and smooth surface (on the microscale) by nature. This fabrication approach immediately rules out the option of an all-quartz chip (option 1 in Table 1), which is optically- and chemically-ideal but technically challenging to fabricate owing to poor machinability of the quartz (quartz−quartz chips require drilling holes for inlet(s) and patterning channels on one of the quartz sides that is only possible with special facilities and tools). As

https://dx.doi.org/10.1021/acs.analchem.9b05734
Anal. Chem. 2020, 92, 2907−2910

our classical CFE devices are made solely of plastic, a logical option to consider was a device with the top and bottom pieces made of a UV-transparent plastic (option 2 in Table 1). UV-transparent plastics, however, have much worse UV transparency than quartz, suggesting a combination of a quartz top piece and a UV-transparent-plastic bottom piece (option 3 in Table 1). While improving the optical quality of the top piece to an ideal level (quartz), this combination does not improve the optical quality of the plastic bottom one. Further, UV transparent plastics give fewer choices for compatibility with organic solvents; in fact, we found only polymethylpentene (PMP) to be suitable for this approach.

The limitations of the transparent-plastic bottom piece suggested embedding a fluorescence layer into the bottom piece as a viable option. Further, self-fluorescence of UV-absorbing plastics, which previously was viewed as an additional optical obstacle, provided a way of "integrating" a fluorescent sublayer with the plastic bottom piece. If the bottom piece is machined from a UV-absorbing visibly fluorescent plastic, then, the top piece could be simply an unprocessed quartz plate (in a PVC-plastic frame) (option 4 in Table 1). Such a device has optical properties even better than those of the quartz−quartz setup due to the absence of any intermediate layer separating the analyte from the fluorescent sublayer. In addition, most UV-absorbing plastics fluoresce in the visible range giving us a good choice of materials for satisfying the requirement of chemical inertness (see the Supporting Information for details).

We fabricated a fully functional CFE chip with a bottom piece made of poly(ether imide) (PEI; a fluorescent plastic) and a top piece made of quartz in a PVC-plastic frame. In essence, the top piece was made out of PVC with a quartz central piece; this central piece functioned as a window (see the Supporting Information for an image). This approach allowed us to use our established protocols for machining plastics while incorporating a quartz window without the need to machine quartz itself. The chip could be imaged with the FSV setup depicted in Figure 2 without an additional fluorescent TLC plate behind the chip.

By using this fully functional quartz−PEI chip, we could clearly see a stream of 100 μM styrene (Figure 3A). The LOD for styrene in this chip was estimated to be 30 μM. In order to assess this LOD, we also fabricated an optically ideal reference device. An optically ideal CFE device for FSV must be made of quartz, the best UV-transparent material. However, making a mesoscale CFE device of pure quartz is technically challenging; we did not have capabilities for making such a device. On the other hand, our imaging experiments for finding the LOD required neither a fully functional nor a pure quartz CFE device. Therefore, we simply emulated an optically ideal CFE device by assembling a pseudodevice with a 200 μm-thick chamber between two quartz plates but without electrodes (Figure 3B). The quartz plates were fixed together by a custom-fabricated plastic frame (see the Supporting Information). The LOD for styrene in this chip was estimated to be 30 μM, i.e., identical to the LOD obtained for the practical CFE device. It is also possible to use the Lambert−Beer law to estimate LOD from a blank measurement (if the extinction coefficient of the analyte is known):

$$\mathrm{LOD} = \frac{1}{\varepsilon_{\mathrm{analyte}} d_{\mathrm{channel}}} \log_{10}\left(\frac{F_{\mathrm{blank}}}{F_{\mathrm{blank}} - 3N}\right) \quad (1)$$

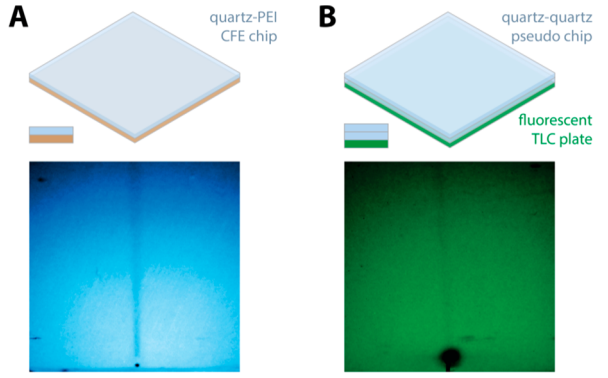

Figure 3. Feasibility of a quartz−PEI CFE chip (A) and a quartz−quartz pseudo chip (B) for FSV. The contrast of both photos was increased to improve visibility of the streams to the human eye. (A) Stream of styrene solution (100 μM) is forwarded into the quartz−PEI CFE chip and visualized by a UV shadow brought onto the fluorescent PEI part. (B) Stream of styrene solution (100 μM) is forwarded into the quartz−quartz pseudo chip and visualized by a UV shadow brought on the fluorescent TLC plate positioned behind the chip.

where F_{blank} is the average fluorescence emission of the nonshaded areas on the chip, N is the noise (= standard deviation of F_{blank}), $\varepsilon_{\mathrm{analyte}}$ is the extinction coefficient of the analyte, and d_{channel} is the depth of the separation zone (see the Supporting Information for details). LOD values for styrene, estimated with eq 1, were between 50 and 250 μM for both the quartz−PEI chip and the quartz−quartz chips. These LODs are widespread and overall greater than the experimental ones, which can be attributed to the nonoptimized excitation light (see the Supporting Information for details) in our setup. Still, these LODs are in the same order of magnitude as the experimentally found ones. All LODs fulfill the requirement of sub-millimolar LODs for our application.

Since the quartz−PEI chip was a fully functional CFI device, we subsequently used it to separate a mixture of benzoic acid and styrene using our established NACFE protocol[6] and detect the streams with FSV. Both molecular streams were clearly visible with the naked eye and detectable with the camera (Figure 4). The streams were evaluated with our "angulagrams" analysis method.[17] Our evaluation revealed that the two

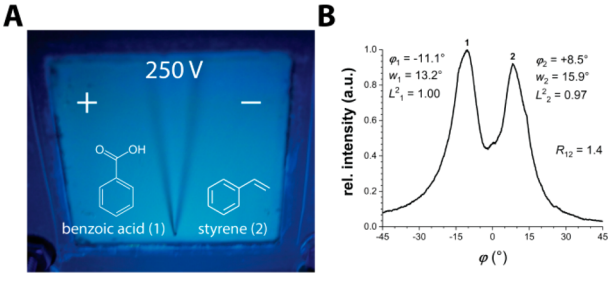

Figure 4. Photo (A) and the angulagram (B) of the separation of benzoic acid (**1**) and styrene (**2**) in CFE. (A) Both streams are clearly visible by naked eye and can be evaluated using our imaging system (Figure 2) using angulagrams. (B) Evaluated angulagram shows the extracted stream parameters (deflection φ, width w, linearity L^2, and resolution R) for benzoic acid and styrene. Conditions: background electrolyte flow rate = 1 mL min^{-1}, sample flow rate = 3 μL min^{-1}, sample concentration = 2.5 mM each in propylene carbonate (see the Supporting Information for more details).

https://dx.doi.org/10.1021/acs.analchem.9b05734
Anal. Chem. 2020, 92, 2907−2910

streams could be separated with a good resolution (R = 1.4) and were highly linear (L^2 > 0.96 for both streams). These results emphasize that not only does the quartz−PEI chip allow FSV in principle but it is also a *practical* CFE device.

In conclusion, we showed that FSV is a feasible and practical approach for visualizing molecular streams in CFE. In this work, we demonstrated the real-time and quantifiable imaging of UV-absorbing small organic molecules with a sub-millimolar LOD that is suitable for integrating CFE into flow chemistry for continuous synthesis and separation. FSV is a very cost-efficient alternative to UV imaging, since FSV requires only a consumer-grade photo/video camera in contrast to a professional-grade UV imaging camera. As FSV is a universal visualization technique, we also foresee applications in the visualization of unlabeled biomolecules such as proteins and DNA in CFE.

■ ASSOCIATED CONTENT

Supporting Information

The Supporting Information is available free of charge at https://pubs.acs.org/doi/10.1021/acs.analchem.9b05734.

Table S1, properties of tested plastic materials; Figure S1, quartz−quartz pseudo device; Figure S2, hybrid PEI−quartz CFE device; Note S1, methods and instrumentation; and Note S2, evaluation procedure (PDF)

■ AUTHOR INFORMATION

Corresponding Author

Sergey N. Krylov − *Department of Chemistry and Centre for Research on Biomolecular Interactions, York University, Toronto M3J 1P3, Canada;* orcid.org/0000-0003-3270-2130; Email: skrylov@yorku.ca

Authors

Nikita A. Ivanov − *Department of Chemistry and Centre for Research on Biomolecular Interactions, York University, Toronto M3J 1P3, Canada*

Sven Kochmann − *Department of Chemistry and Centre for Research on Biomolecular Interactions, York University, Toronto M3J 1P3, Canada;* orcid.org/0000-0001-7423-4609

Complete contact information is available at: https://pubs.acs.org/10.1021/acs.analchem.9b05734

Author Contributions

The manuscript was written through contributions of all authors.

Notes

The authors declare no competing financial interest.

■ ACKNOWLEDGMENTS

This work was supported by the Natural Sciences and Engineering Research Council of Canada (Grant STPG-P 521331-2018).

■ REFERENCES

(1) Castro, E. R.; Manz, A. *J. Chromatogr. A* **2015**, *1382*, 66−85.
(2) Novo, P.; Janasek, D. *Anal. Chim. Acta* **2017**, *991*, 9−29.
(3) Johnson, A. C.; Bowser, M. T. *Lab Chip* **2018**, *18*, 27−40.
(4) Britton, J.; Raston, C. L. *Chem. Soc. Rev.* **2017**, *46*, 1250−1271.
(5) Suryawanshi, P. L.; Gumfekar, S. P.; Bhanvase, B. A.; Sonawane, S. H.; Pimplapure, M. S. *Chem. Eng. Sci.* **2018**, *189*, 431−448.
(6) Ivanov, N. A.; Liu, Y.; Kochmann, S.; Krylov, S. N. *Lab Chip* **2019**, *19*, 2156−2160.
(7) Rudisch, B. M.; Pfeiffer, S. A.; Geissler, D.; Speckmeier, E.; Robitzki, A. A.; Zeitler, K.; Belder, D. *Anal. Chem.* **2019**, *91*, 6689−6694.
(8) Turgeon, R. T.; Bowser, M. T. *Electrophoresis* **2009**, *30*, 1342−1348.
(9) Köhler, S.; Nagl, S.; Fritzsche, S.; Belder, D. *Lab Chip* **2012**, *12*, 458−463.
(10) Kochmann, S.; Krylov, S. N. *Lab Chip* **2017**, *17*, 256−266.
(11) Nagl, S. *Engineering* **2018**, *18*, 114−123.
(12) Saar, K. L.; Zhang, Y.; Müller, T.; Kumar, C. P.; Devenish, S.; Lynn, A.; Łapińska, U.; Yang, X.; Linse, S.; Knowles, T. P. J. *Lab Chip* **2018**, *18*, 162−170.
(13) Pfeiffer, S. A.; Rudisch, B. M.; Glaeser, P.; Spanka, M.; Nitschke, F.; Robitzki, A. A.; Schneider, C.; Nagl, S.; Belder, D. *Anal. Bioanal. Chem.* **2018**, *410*, 853−862.
(14) Anciaux, S. K.; Bowser, M. T. *Electrophoresis* **2019**, DOI: 10.1002/elps.201900179.
(15) Song, Y.-A.; Chan, M.; Celio, C.; Tannenbaum, S. R.; Wishnok, J. S.; Han, J. *Anal. Chem.* **2010**, *82*, 2317−2325.
(16) Benz, C.; Boomhoff, M.; Appun, J.; Schneider, C.; Belder, D. *Angew. Chem., Int. Ed.* **2015**, *54*, 2766−2770.
(17) Kochmann, S.; Agostino, F. J.; LeBlanc, J. C. Y.; Krylov, S. N. *Anal. Chem.* **2016**, *88*, 8415−8420.
(18) Brockmann, H.; Volpers, F. *Chem. Ber.* **1947**, *80*, 77−82.
(19) Sease, J. W. *J. Am. Chem. Soc.* **1947**, *69*, 2242−2244.
(20) Hassur, S. M.; Whitlock, H. W. *Anal. Biochem.* **1974**, *59*, 162−164.
(21) Meyers, C. L. F.; Meyers, D. J. *Curr. Protoc. Nucleic Acid Chem.* **2008**, *34*, A.3D.1−A.3D.13.
(22) Hollenstein, M.; Damha, M. J. *Curr. Protoc. Nucleic Acid Chem.* **2016**, *67*, 7.26.1−7.26.15.
(23) Herrera, R. E.; Shaw, P. E. *Nucleic Acids Res.* **1989**, *17*, 8892.
(24) Thurston, S. J.; Saffer, J. D. *Anal. Biochem.* **1989**, *178*, 41−42.
(25) Kochmann, S.; Krylov, S. N. *Anal. Chem.* **2018**, *90*, 9504−9509.